A discussion on the apparently puzzling structural, electrical and magnetic properties of BaVS$_3$

M.-H. Whangbo,[a,*] H.-J. Koo,[a] D. Dai,[a] and A. Villesuzanne[b]

[a] Department of Chemistry, North Carolina State University, Raleigh, NC 27695-8204, USA
[b] ICMCB-CNRS, 87, avenue du Dr. A. Schweitzer, 33608 Pessac Cedex, France

Abstract

The ternary vanadium sulfide BaVS$_3$ consists of VS$_3$ chains made up of face sharing VS$_6$ octahedra, and exhibits a number of structural, electrical and magnetic properties that are not explained in terms of the normal metallic state. Our analysis indicates that the spin ordering of BaVS$_3$ taking place below 30 K is most probably random along the chain direction. Thus the puzzling properties of BaVS$_3$ are explained in terms of the broken-symmetry electronic state in which pairs of nonmagnetic V atoms alternate with those of magnetic V atoms in each VS$_3$ chain. The origin of this broken-symmetry state was discussed on the basis of cooperative Jahn–Teller distortion and lattice strain.
© 2003 Elsevier Inc. All rights reserved.

1. Introduction

Ternary vanadium sulfide BaVS$_3$ exhibits unusual electrical and magnetic properties [1–8]. Upon lowering the temperature BaVS$_3$ undergoes three phase transitions; a structural transition at $T_S \approx 240$ K, a metal–insulation (MI) transition at $T_{MI} \approx 70$ K, and a magnetic transition at $T_X \approx 30$ K. In the room temperature structure of this compound, VS$_3$ chains made up of face-sharing VS$_6$ octahedra have a hexagonal arrangement with Ba^{2+} ions filling the channels formed by every three chains (Fig. 1) [9, 10]. Despite this one-dimensional (1D) nature of the structure, the electrical resistivity of BaVS$_3$ is not highly anisotropic but is rather three dimensional (3D) [6]. The electrical resistivity of BaVS$_3$ is nearly independent of temperature above T_{MI} and increases sharply below T_{MI} [1, 6].

The magnetic susceptibility of BaVS$_3$ follows a Curie–Weiss behavior above T_{MI} with the reported μ_{eff} values ranging 1.17–1.33 μ_B [2, 11–13], which amounts to 0.54–0.66 unpaired spin per V. The magnetic susceptibility decreases rapidly below T_{MI} [1, 2, 6] without any long-range magnetic order between T_X and T_{MI} [5]. An incommensurate antiferromagnetic spin structure sets in below T_X with the ordered magnetic moment of $\sim 0.5 \mu_B$

and the propagation vector $q_{spin} = (0.226a^*, 0.226b^*, 0)$ in the hexagonal setting [5]. Thus the V^{4+} (d^1) sites of BaVS$_3$ are grouped into magnetic and nonmagnetic sites in approximately 1:1 ratio [8, 12, 14], and the c-axis length of the ordered spin structure is apparently the same as that of the room temperature crystal structure (i.e., the c^* component of q_{spin} is zero).

A powder neutron diffraction study [10] reported that the V^{4+} (d^1) ions of each VS$_3$ chain form a straight chain at room temperature, but a zigzag chain below T_S. Each VS$_3$ chain has two equivalent V atoms per unit cell in both structures. However, a recent X-ray diffraction study [8] of single crystal BaVS$_3$ samples found that there occur superlattice reflections with propagation vector $0.5c^*$ below T_{MI}. Thus, the MI transition involves a spatial order of the lattice and doubles the c-axis length. This work showed that the correct space group for the structure of BaVS$_3$ below T_{MI} is not $Cmc2_1$ [10], but is likely to be $Im2m$ in which two nonequivalent V atoms (say, V$_A$ and V$_B$) repeat as $-V_A-V_A-V_B-V_B-V_A-V_A-V_B-V_B-$ in each VS$_3$ chain. Subsequently, it was observed [15] that the MI transition of BaVS$_3$ is accompanied by huge 1D structural fluctuations (observable up to 170 K) reminiscent of a pseudo 1D metal.

The properties of BaVS$_3$ present a number of puzzling features. The observed electrical resistivity does not exhibit 1D metallic character [6] despite that it consists

*Corresponding author. Fax: +919-515-7832.
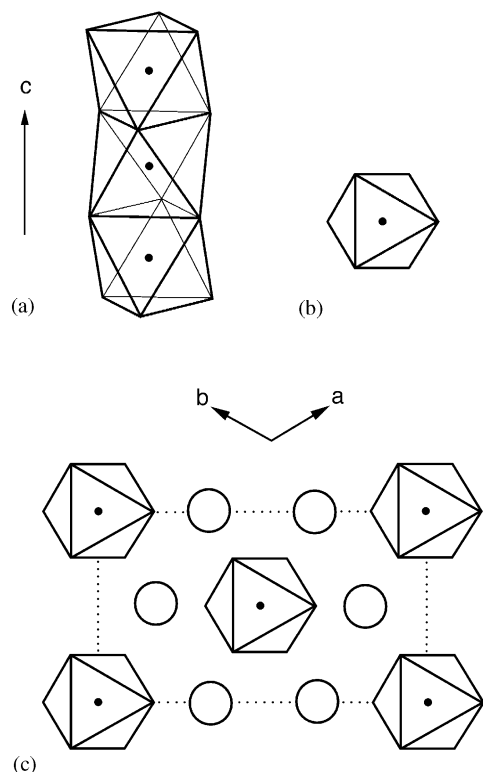E-mail address: mike_whangbo@ncsu.edu (M.-H. Whangbo).

Fig. 1. Description of the room-temperature crystal structure of $BaVS_3$: (a) Perspective view of a VS_3 octahedral chain. (b) Projection view of a VS_3 chain along the chain direction. (c) Projection view, along the c-direction, of the arrangements of the VS_3 chains. The dots and open circles represent the V^{4+} and Ba^{2+} ions, respectively. The rectangle of dotted lines in (c) represents a unit cell of the orthorhombic structure below T_S.

of 1D chains. Nevertheless, $BaVS_3$ exhibits strong 1D structural fluctuations as if it is a 1D metal. The MI transition doubles the c-axis length in terms of the crystal structure, but the ordered spin structure below T_X appears to have the same c-axis length as does the room temperature crystal structure. With an array of V^{4+} (d^1) ions in each VS_3 chain, one might expected a Peierls distortion leading to a $V-V \cdots V-V \cdots$ bond alternation, but this does not happen. It is clear why the ordered spin structure below T_X is incommensurate in the ab-plane. In the present work we examine probable causes for these apparently puzzling observations.

2. Normal metallic state and charge density wave

The normal metallic state of a 1D metal consisting of 1D chains is represented by the electron configuration in which the band levels are each doubly occupied up to the Fermi level. The partially filled band associated with such a band filling gives rise to a charge density wave (CDW) instability. The latter induces a periodic lattice distortion (PLD) with propagation vector $2k_F$, where k_F is the Fermi wave vector. The PLD opens a band gap at

the Fermi level, and eventually leads to an MI transition below a certain temperature T_p [16]. For the distorted structure below T_p, the $2k_F$ value is equal to the distance q from a plane of Bragg reflections to that of the adjacent superlattice spots [17]. Above T_p a CDW instability induces 1D structural fluctuations (i.e., regions of short-range PLD are formed and destroyed dynamically in individual chains), which give rise to diffuse spots between the Bragg reflections [17]. For the undistorted structure above T_p, the $2k_F$ value is related to the occupancy f of the partially filled band causing the CDW instability. For example, if the chains of a pseudo 1D metal are aligned along the c-direction, the occupancy f of its partially filled band is given by $f = q/c^* = 2k_F/c^*$ [16].

The 1D structural fluctuations and the superlattice spots of $BaVS_3$ are characterized by the propagation vector $q = 0.5c^*$ [8, 15]. For these 1D structural fluctuations to originate from a CDW instability, $BaVS_3$ should have a half-filled band dispersive mainly along the chain direction (i.e., the c-direction) and the associated Fermi surface should be well nested [16]. These expectations are not supported by the results of the first principles electronic band structure calculations for the normal metallic state of the room temperature structure of $BaVS_3$ [7, 18]: the partially filled band dispersive along the c^*-direction has strong contributions of the $3z^2 - r^2$ orbitals of V, has a folded structure due to the presence of two V atoms per unit in each VS_3 chain, and the lower branch of this folded band is almost completely filled rather than half filled. The associated Fermi surface (Fig. 2), determined on the basis of the full potential linearized augmented plane wave (FP-LAPW) calculations [19] reported earlier [7], is so strongly warped that it cannot induce any CDW instability. Therefore, the 1D structural fluctuations of
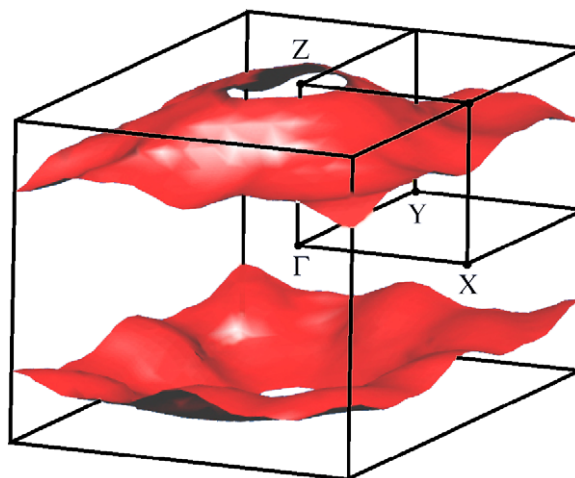

Fig. 2. Fermi surface associated with the partially filled band (dispersive along the chain direction) calculated for the normal metallic state of $BaVS_3$ by FP-LAPW calculations. $\Gamma = (0, 0, 0)$, $X = (0.5a^*, 0, 0)$, $Y = (0, 0.5b^*, 0)$, $Z = (0, 0, 0.5c^*)$.

$BaVS_3$ cannot be explained in terms of its normal metallic state.

3. Models of broken-symmetry electronic states

The magnetic properties of $BaVS_3$ show that there is 0.54–0.66 spin/V above T_{MI}, and about 0.5 spin/V below T_X. For the discussion of the electronic structure of $BaVS_3$ above T_{MI}, therefore, it is more appropriate to begin from the viewpoint of an electron-localized state in which each V^{4+} site has one localized spin. If the correct space group of $BaVS_3$ is $Im2m$ below T_{MI}, as deduced by Inami et al. [8], two nonequivalent V atoms repeat as $(-V_A-V_A-V_B-V_B-)_\infty$ in each VS_3 chain so that the c-axis doubling comes about naturally. To explain the structural and magnetic properties of $BaVS_3$ under the constraint that the V^{4+} (d^1) ions are separated into magnetic and nonmagnetic sites in approximately 1:1 ratio, two symmetry-broken electronic structures have been proposed [8, 15].

Inami et al. [8] considered the possibility state two electrons in one pair of vanadium (e.g., V_A-V_A) form a singlet ground state, and those in the other pair (e.g., V_B-V_B) are localized (Model 1) (Fig. 3a). The t_{2g} levels of a VS_6 octahedron can be described by employing either the symmetry-adapted or symmetry-broken t_{2g} orbitals [7]. As Fagot et al. [15] suggested it is reasonable to suppose that the V_A sites utilize the $3z^2 - r^2$ orbitals (symmetry-adapted). These orbitals will produce a σ-bonding level and accommodate two electrons forming a singlet ground state so that each V_A-V_A pair becomes nonmagnetic. For the V_B sites to be magnetic, symmetry-broken t_{2g} orbitals are more effective than the symmetry-adapted $e(t_{2g})$ orbitals because the former diminishes orbital overlap between adjacent V sites (Fig. 3a) [7]. The spin structure of Model 1 doubles the c-axis length, in apparent disagreement with the ordered spin structure deduced from powder neutron diffraction
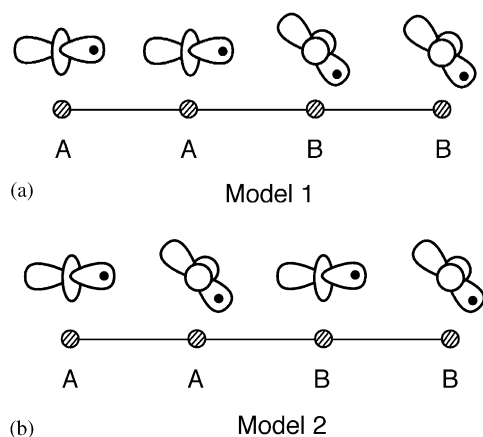

Fig. 3. Two broken-symmetry electronic states of a VS_3 chain, where the V atoms are represented by shaded circles.

[5]. Fagot et al. [15] considered an alternative possibility that every second V atom along each chain has one electron in the $3z^2 - r^2$ orbital, and each of the remaining V atoms has a localized spin (Model 2) (Fig. 3b). This model does not double the c-axis as far as the spin structure is concerned, but is incompatible with the space group $Im2m$, because it generates four nonequivalent V atoms (i.e., two different V_A and two different V_B atoms).

It should be recalled that ferromagnetic ordering along the c-direction (i.e., the c^* component of q_{spin} is zero) was not deduced experimentally, but was rather assumed to determine the propagation vector in the ab-plane from the powder neutron diffraction data [5]. Therefore, it is critical to know if Model 1 is consistent with the vector q_{spin} thus determined. For this purpose, we first consider the possible nature of spin ordering in the ab-plane.

A 3D arrangement of VS_3 chains appropriate for Model 1 is one in which two consecutive sheets of V_AS_6 octahedra (parallel to the ab-plane) alternate with two consecutive sheets of V_BS_6 octahedra along the c-direction. In $BaVS_3$ each Ba atom is located at the center of a V_6 trigonal prism. The above 3D arrangement of VS_3 chains generates four BaV_6 trigonal prisms for every $V_A-V_A-V_B-V_B$ unit, i.e., one $Ba(V_A)_6$, one $Ba(V_B)_6$ and two $Ba(V_A)_3(V_B)_3$. This is consistent with the expected Ba positions from the space group $Im2m$ [8]. Suppose that each V_A-V_A pair along the chain direction forms a σ-bonding level, and the unpaired spins in each sheet of V_BS_6 octahedra order through super-superexchange interactions in the ab-plane [7]. The decrease of the magnetic susceptibility below T_{MI} and the lack of long-range spin order between T_{MI} and T_X are explained in terms of random arrangements of antiferromagnetically coupled interchain spin dimers $(V_BS_6)_2$ within the sheets of V_BS_6 octahedra (Fig. 4a) [6, 7]. In this picture, the occurrence of an ordered incommensurate spin structure in each sheet of V_BS_6 octahedra should be a consequence of ordering such spin dimers. Fig. 4b shows an example of a $\sqrt{21} \times \sqrt{21}$ superstructure with repeat vectors $\mathbf{a'} = 5\mathbf{a} + \mathbf{b}$ and $\mathbf{b'} = 4\mathbf{b} - \mathbf{a}$ (here $\mathbf{a}$ and $\mathbf{b}$ are the repeat vectors of the hexagonal room temperature structure). The propagation vector of this superstructure in reciprocal space is $(0.218a^*, 0.218b^*)$, which is close to that of the reported incommensurate structure, i.e., $(0.226a^*, 0.226b^*)$ [5].

The 3D spin structure of $BaVS_3$ below T_X can be described in terms of ordering, along the c-direction, the $\sqrt{21} \times \sqrt{21}$ superstructures formed in the sheets of V_BS_6 octahedra. Spin exchange interactions along the c-direction are possible between adjacent sheets of V_BS_6 octahedra joined by face sharing, but not between those separated by sheets of V_AS_6 octahedra. Along the c-direction, therefore, the $\sqrt{21} \times \sqrt{21}$ superstructures formed in the sheets of V_BS_6 octahedra would propagate
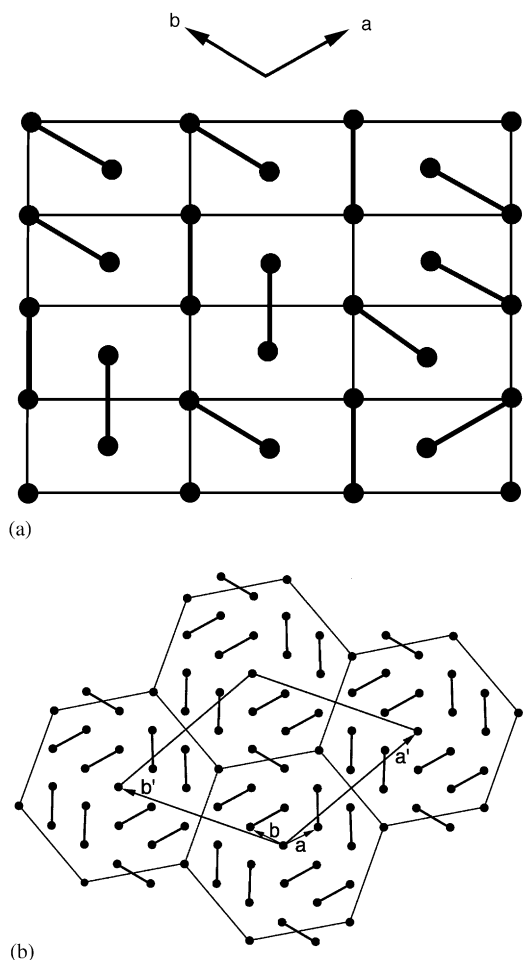
Fig. 4. (a) Random arrangement of antiferromagnetically coupled interchain spin dimers (represented by solid lines) within a layer of VS_6 octahedra parallel to the *ab*-plane. (b) $\sqrt{21} \times \sqrt{21}$ superstructure of spin dimer ordering. The dots represent the V^{4+} ion positions.

without any repeat pattern. Powder neutron diffraction patterns for such a random ordering would be well described by the assumption that the c^* component of the propagation vector is zero. Thus, Model 1 is consistent with the vector $q_{spin} = (0.226a^*, 0.226b^*, 0)$ if the spin ordering along the *c*-direction is random.

4. Discussion

Since the properties of $BaVS_3$ are explained in terms of the broken-symmetry electronic state, Model 1, it is important to ask why such a state can become the ground state to begin with. For our discussion, it is necessary to consider two opposing energy factors, i.e., lattice strain and cooperative Jahn–Teller distortion.

$BaVS_3$ has a close packed hexagonal arrangement of VS_3 chains, and each Ba^{2+} ion is located in a pocket of 12 S atoms in the channels created by three adjacent chains. In addition, the nearest-neighbor V–V distance

of the VS_3 chain is very short (i.e., 2.805 Å) due to the face sharing. In this compact structure, a V–V···V–V··· bond alternation along the chain is energetically unfavorable because it forces a change in the V–S bond lengths and a shortening of the Ba–S contact distances and hence leads to severe lattice strain. Model 1 requires every fourth V–V pair of each chain to form a V–V σ-bonding level and induces less severe lattice strain than does the V–V···V–V··· bond alternation.

The V^{4+} (d^1) ion of each VS_6 octahedron has Jahn–Teller instability. The crystal structures of $BaVS_3$ determined below T_S [10] suggest that the preferred distortion for lifting the t_{2g} level degeneracy is one in which the V atom of each VS_6 octahedron moves toward one S_3 triangle face. Then, at a given VS_6 octahedron of a VS_3 chain, the V atom can move toward a shared face along the chain or toward triangular faces in the direction perpendicular to the chain. In each V_A–V_A pair, it is energetically favorable for the V_A atoms to move toward each other along the chain and form a σ-bonding level. In order to avoid strong lattice strain, the V_B atoms in each V_B–V_B pair cannot follow the same distortion pattern. Then the V_B atoms should move either away from each other along the chain or in the direction perpendicular to the chain. Thus, in a V_B–V_B pair, shortening of the V_B–V_B distance and formation of a σ-bonding are prevented so that the V_B atoms remain magnetic.

The symmetry-broken state, Model 1, should arise as a consequence of balancing two opposing energy terms, i.e., stabilization from cooperative Jahn–Teller distortions and destabilization from the associated lattice strain. In terms of Model 1, the 1D structural fluctuations in $BaVS_3$ mean that regions of short-range cooperative Jahn–Teller distortions are formed and destroyed dynamically in individual VS_3 chains. The 1D structural fluctuations in each VS_3 chain will reduce the mean free path, and lower the mobility, of electrons mainly along the chain direction. Thus strong 1D metallic conductivity is absent in $BaVS_3$.

5. Concluding remarks

Our work indicates that the structural and physical properties of $BaVS_3$ are not explained by the normal metallic state, but by the broken-symmetry electronic state, Model 1, and that the spin ordering below T_X is random along the *c*-direction. The lattice distortion accompanying the MI transition of $BaVS_3$ represents a cooperative Jahn–Teller distortion. When regions of cooperative Jahn–Teller distortions are formed and destroyed dynamically in individual VS_3 chains, there should occur 1D structural fluctuations. The latter should reduce electrical conductivity preferentially along

the chain direction so that strong 1D metallic conductivity is absent in $BaVS_3$.

Acknowledgments

The work at North Carolina State University was supported by the Office of Basic Energy Sciences, Division of Materials Sciences, US Department of Energy, under Grant DE-FG02-86ER45259. The computational work at ICMCB was aided by the M3PEC project (Modélisation Microscopique et Mésoscopique en Physique, dans l'Environnement et en Chimie), Université de Bordeaux I. M.-H. W. thanks Dr. P. Foury-Leylekian, Dr. J. Köhler and Dr. C. C. Torardi for invaluable discussions.

References

[1] M. Nakamura, A. Sekiyama, H. Namatame, A. Fujimori, H. Yoshihara, T. Ohtani, A. Misu, M. Takano, Phys. Rev. B 49 (1994) 16191.

[2] T. Graf, D. Mandrus, J.M. Lawrence, J.D. Thompson, P.C. Canfield, S.-W. Cheong, L.W. Rupp Jr., Phys. Rev. B 51 (1995) 2037.

[3] H. Nakamura, H. Imai, M. Shiga, Phys. Rev. Lett. 79 (1997) 3779.

[4] H. Nakamura, H. Tanahashi, H. Imai, M. Shiga, K. Kojima, K. Kakurai, M. Nishi, J. Phys. Chem. Solids 61 (1999) 1137.

[5] H. Nakamura, T. Yamasaki, S. Giri, H. Imai, M. Shiga, K. Kojima, M. Hishi, K. Kakurai, N. Metoki, J. Phys. Soc. Jpn. 69 (2000) 2763.

[6] G. Mihály, I. Kézsmárki, F. Zámborsky, M. Miljak, K. Penc, P. Fazekas, H. Berger, L. Forró, Phys. Rev. B 61 (2000) R7831.

[7] M.-H. Whangbo, H.-J. Koo, D. Dai, A. Villesuzanne, J. Solid State Chem. 165 (2002) 345.

[8] T. Inami, K. Ohwada, H. Kimura, M. Watanabe, Y. Noda, H. Nakamura, T. Yamasaki, M. Shiga, N. Ikeda, Y. Murakami, Phys. Rev. B 66 (2002) 073108.

[9] R.A. Gardner, M. Vlasse, A. Wold, Acta Crystallogr. B 25 (1969) 781.

[10] M. Ghedira, M. Anne, J. Chenavas, M. Marezio, F. Sayetat, J. Phys. C: Solid State Phys. 19 (1986) 6489.

[11] O. Massenet, R. Buder, J.J. Since, C. Schlenker, J. Mercier, J. Kelber, G.D. Stucky, Mater. Res. Bull. 13 (1978) 187.

[12] H. Nishihara, M. Takano, J. Phys. Soc. Jpn. 50 (1981) 426.

[13] K. Matsuhara, T. Wada, T. Nakamizo, H. Yamauchi, S. Tanaka, Phys. Rev. B 43 (1991) 13118.

[14] A. Heidemann, M. Takano, Phys Stat. Sol. B 100, (1980) 343.

[15] S. Fagot, P. Foury-Leylekian, S. Ravy, J.-P. Pouget, H. Berger, Phys. Rev. Lett. 90 (2003) 196401.

[16] M.-H. Whangbo, E. Canadell, J. Am. Chem. Soc. 114 (1992) 9587.

[17] R. Moret, J.-P. Pouget, in: J. Rouxel (Ed.), Crystal Chemistry Properties of Materials with Quasi-One-Dimensional Structures, Reidel, Dordrecht, The Netherlands, 1986, p. 87.

[18] L.F. Mattheiss, Solid State Commun. 93 (1995) 791.

[19] P. Blaha, K. Schwarz, G. Madsen, D. Kvasnicka, J. Luitz, WIEN2k, An Augmented Plane Wave + Local Orbitals Program for Calculating Crystal Properties, Karlheinz Schwarz, Techn. Universität Wien, Austria, 2001, ISBN 3-9501031-1-2, see also: http://www.wien2k.at/